Morini and da Cunha
Surgical and Experimental Pathology (2024) 7:23
https://doi.org/10.1186/s42047-024-00166-0

Surgical and Experimental Pathology

REVIEW

Open Access

Navigating the complexity of Wilms tumors in pediatrics: diagnostic challenges for better treatment

Mariana Andozia Morini[1*] and Isabela Werneck da Cunha[1]

Abstract

Most pediatric kidney tumors clinically present as an abdominal mass, typically detected by the child's caregivers and later confirmed through imaging tests. Malignant renal cancers account for approximately 5% of childhood kidney neoplasms, with Wilms tumors (WT) being the most common diagnosis in this category (90% of cases).

Patients are treated according to two main protocols: the American protocol of the Children's Oncology Group (COG) or the protocol from the Société Internationale d'Oncologie Pédiatrique (SIOP), which differ in terms of the timing of surgery (before or after chemotherapy).

Grossly, pediatric kidney tumors are neoplasms that can vary significantly in size. After a correct histological diagnosis, the child will be treated according to the guidelines for that specific neoplasm. Therefore, the accurate diagnosis of the histological subtype is crucial for determining the appropriate treatment that can improve survival rates in children. Consequently, it is extremely important to recognize neoplasms that require differentiation from WT.

Keywords Wilms tumors differential diagnosis, Pediatric renal tumors, Wilms tumor, Pathology, Review, Brazilian kidney tumors group

Background

Most pediatric kidney tumors manifest clinically as an abdominal mass, usually detected by the child's caregivers and later confirmed through imaging tests, followed by a chemotherapy or surgery. Since Wilms tumors (WT) are the most common renal neoplasm in childhood—generally affecting children with an average age of 3 years [1] —they have an overall five-year survival rate that can reach 90% in individuals under 15 years of age. Therefore, early diagnostic is essential.

Clinically, a palpable abdominal mass is detected, which may be unilateral or bilateral (5–10% bilateral or multicentric). However, some patients may already have metastases, primarily to the lungs. Complementary imaging tests (abdominal ultrasound, computed tomography, and magnetic resonance imaging) help confirm the diagnostic hypothesis. Patients are treated according to one of the two main protocols: the protocol of the Children's Oncology Group (COG), which consists of a biopsy followed by surgery without neoadjuvant chemotherapy in most cases, or the treatment based on the Société Internationale d'Oncologie Pédiatrique (SIOP) protocol, which includes neoadjuvant chemotherapy for any child with renal masses suspected clinically and radiologically to be Wilms tumor. This neoadjuvant treatment aims to necrotize and shrink the tumor [2] by reducing the proportion of certain histological components of the neoplasm, primarily the blastema component.

Grossly, pediatric kidney tumors can vary significantly in size, potentially forming large abdominal masses that

*Correspondence:
Mariana Andozia Morini
mariana.matushita@rededor.com.br
[1] Instituto D'Or de Pesquisa e Ensino (IDOR), São Paulo, Brazil

deform the kidney. The appearance of tumors may be very heterogeneous due to the different components, which is also a clue for definitive diagnosis. WT can exhibit viable areas (grayish in color and elastic in consistency), as well as hemorrhagic, necrotic, or cystic components, depending on the response to chemotherapy. Therefore, the representation of the tumor by the pathologist is of fundamental importance to adequately represent the neoplasm, given its heterogeneity. The SIOP protocol [3] recommends that the surgical specimen be representative of the tumor in its largest extent, and that this largest tumor slice be mapped for adequate microscopic representation of the different tumor components and their fundamental anatomical areas in the assessment of staging and risk classification of renal tumors.

Histologically, Wilms tumors (WT) comprise three main histological patterns: epithelial, mesenchymal/stromal, and undifferentiated (blastema), which can be present in varying amounts. Not all three components must be present; some Wilms tumors can be biphasic or monophasic. In cases where only one pattern is observed, differential diagnosis and confirmation with complementary tests such as immunohistochemistry and molecular studies are recommended.

Due to their rarity, general pathologists may have difficulty recognizing these tumors, as various other tumors can simulate WT. Therefore, understanding the differential diagnosis is crucial for the effective treatment of these tumors, highlighting the importance of trained pathologists in pediatric and childhood neoplasia.

The child's risk classification occurs after the histological evaluation of the surgical specimen by the pathologist. This classification fundamentally depends on the accurate quantification of each histological component present in the tumor, categorizing them into three risk categories: low, intermediate, or high risk (see Table 1). Cases with predominancy of blastema are considerate high risk, while epithelial, stromal and mixed type are intermediate risk. Cases where we have completely response after chemotherapy are considerate low risk as well as another histologic subtype as Cystic partially differentiated nephroblastoma (CPDN) and mesoblastic nephroma. It's important to note that the presence of diffuse anaplasia, despite the amount of any component, are considerate high risk.

Among the difficulties faced by non-specialist pathologists, improper histological classification and imprecise risk stratification can lead to altered treatment plans, resulting in worse prognosis and outcomes. The lack of standardization in the macroscopic examination of the surgical specimen may be one of the primary reasons for inadequate treatment.

Since the different histological patterns found in WT can be mistaken for several other tumors, we will discuss the main differential diagnoses based on each histological component (epithelial, mesenchymal, or blastema).

Microscopy of Wilms tumors (WT)

Epithelial pattern of WT

The epithelial pattern of Wilms tumors (WT) consists of epithelial structures that alternate between tubules and glomerular formations, varying from primitive (Fig. 5) to well-differentiated epithelium (Figs. 1, 2, 3, 4). The cells are columnar, with hyperchromatic and elongated nuclei, an inconspicuous nucleolus, and scant cytoplasm. The differential diagnosis of the epithelial component includes epithelial tumors or lesions such as nephrogenic rests, metanephric adenoma, and renal cell carcinoma, primarily papillary renal cell carcinoma. The primitive epithelial component, which is poorly differentiated, can be differentiated from the blastema pattern (Fig. 5).

Stromal/mesenchymal pattern of WT

Stromal pattern of Wilms tumors usually consists of spindle cells arranged in long or short bundles or in a storiform pattern (Figs. 6 and 7). It can also be present as solid or myxoid areas [4].

Heterologous components are common findings, with rhabdomyoblastic differentiation being the most

Table 1 Risk classification of Wilms tumors according to the histological subtype of the neoplasm

Low risk	Cystic partially differentiated nephroblastoma	**High risk**	Blastema
	Completely necrotic		Diffuse anaplasia
	Mesoblastic nephroma		
Intermediate risk	Non anaplasic and variants	**Others**	Clear cell sarcoma of the kidney
	Epithelial WT		Malignant rhabdoid tumor
	Stromal WT		Renal cell carcinoma
	Mixed WT		Others
	Regressive WT		Indeterminate
	Focal anaplasia		Nephroblastomatosis

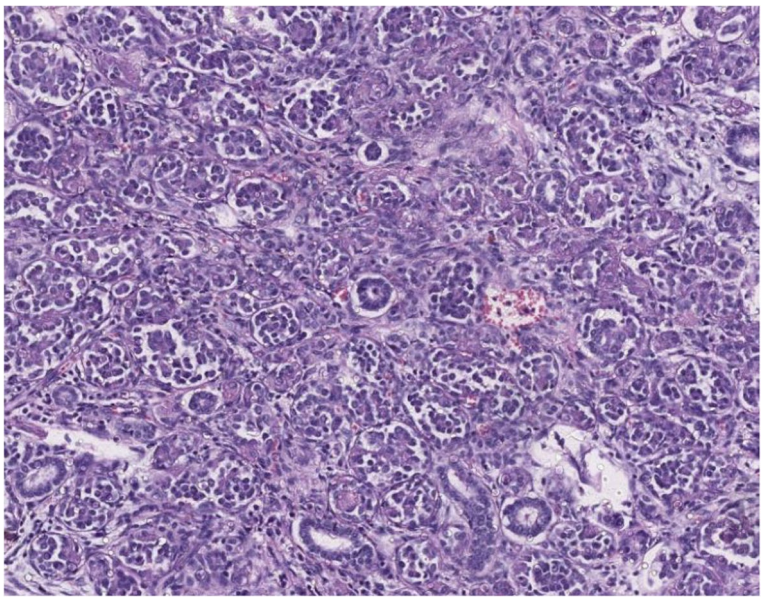

Fig. 1 Epithelial component of WT; tubules and glomerular formations that vary from poor to well differentiated. The cells are columnar, with hyperchromatic and elongated nuclei, an inconspicuous nucleolus and scant cytoplasm

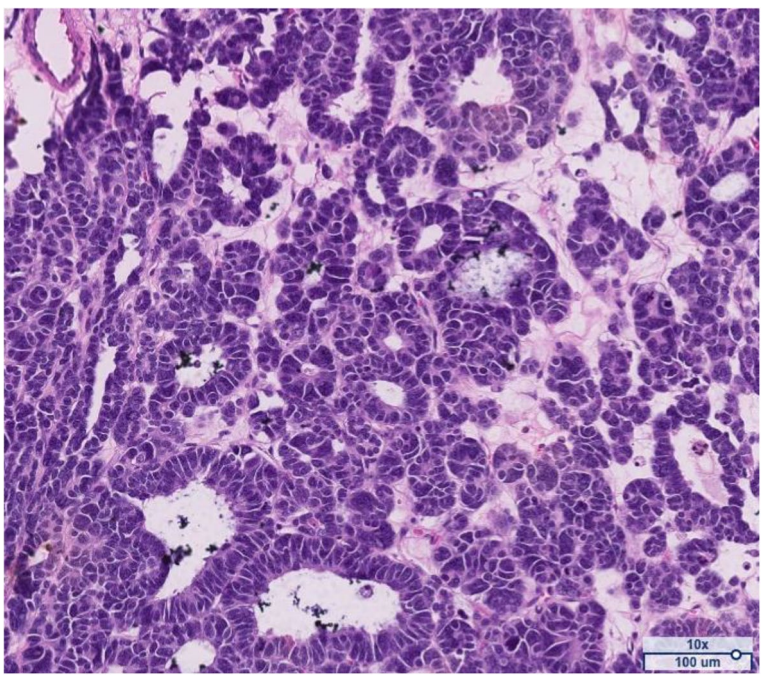

Fig. 2 WT epithelial component; epithelial structures that alternate between tubules and glomerular formations that vary from poor to well differentiated. The cells are columnar, with hyperchromatic and elongated nuclei, an inconspicuous nucleolus and scant cytoplasm

prevalent (Fig. 8), although other components such as bone, cartilage, and adipose tissue may also be present (Fig. 9).

In some cases, WT may have the stromal pattern as its major component, and recognizing epithelial or blastema components, even in small amounts, aids in its diagnosis. When the stromal component is the only one present,

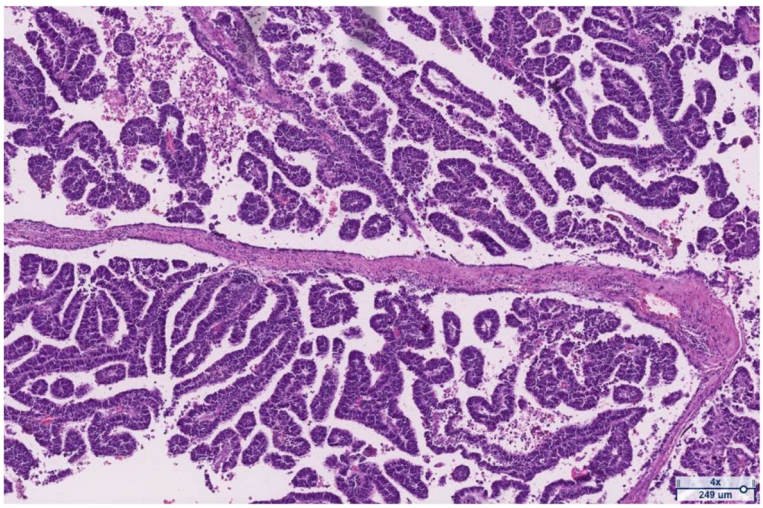

Fig. 3 Pseudopapillae formation in epithelial WT simulating Papillary renal cell carcinoma.

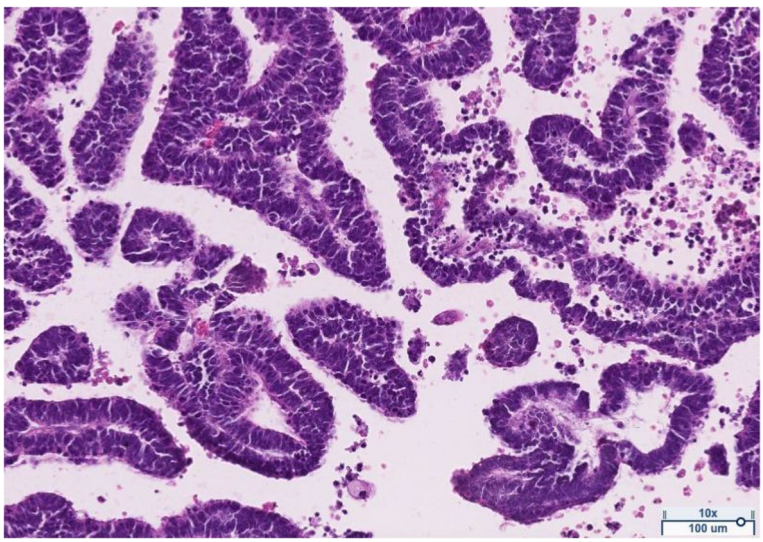

Fig. 4 Pseudopapillae formation in epithelioid WT (10x)

identifying nephrogenic rests is crucial for diagnosing WT.

There are other kidney tumors with fusiform cellular aspects that can be mistaken for the stroma of WT. Among these, clear cell sarcoma of the kidney, congenital mesoblastic nephroma, and metanephric stromal tumor are the most common.

Anaplasia and pseudo-anaplasia

The stromal/mesenchymal pattern often exhibits what is referred to as pseudoanaplasia (Fig. 10), characterized by cells, primarily rhabdomyoblasts, which display intense pleomorphism, multinucleation, and hyperchromasia. These features can easily be confused with true anaplasia. It is crucial to distinguish pseudoanaplasia from anaplasia, as anaplastic Wilms tumors have a worse prognosis and consequently require a more aggressive treatment approach. Atypical mitoses must be present in pleomorphic areas for a diagnosis of anaplasia. Furthermore, anaplasia generally shows expression of p53 when assessed by immunohistochemistry [4] (Fig. 11).

Anaplasia can also be stratified into diffuse or focal categories based on its extent. Diffuse anaplasia is defined as anaplastic areas measuring more than 1.5 mm or present in more than two slides (i.e., more than two foci). Focal anaplasia is defined by an anaplastic area that does not exceed 1.5 mm [5–7].

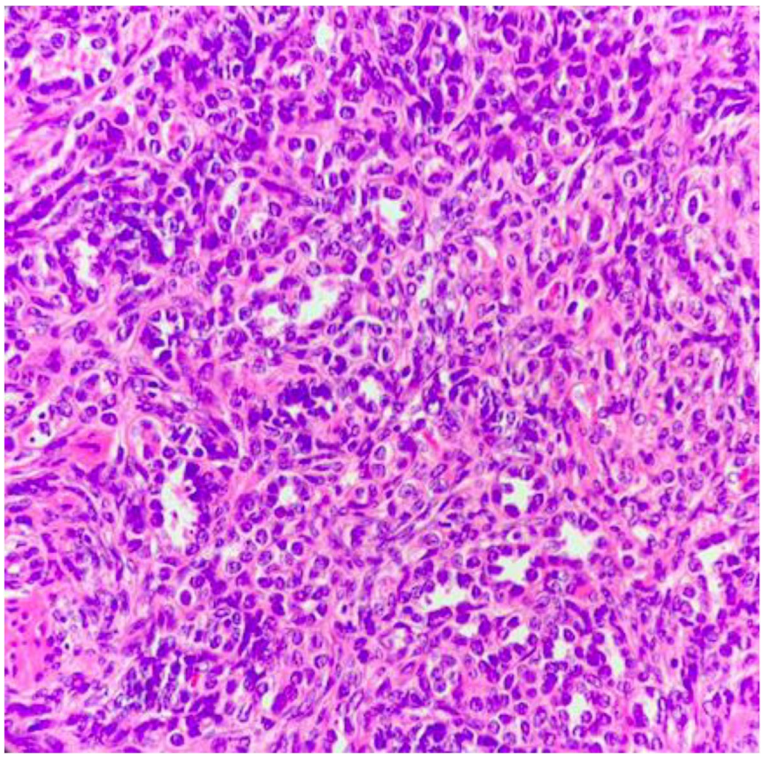

Fig. 5 Primitive epithelial pattern, with initial tubular differentiation. In this case, it can be mistake with blastematous pattern

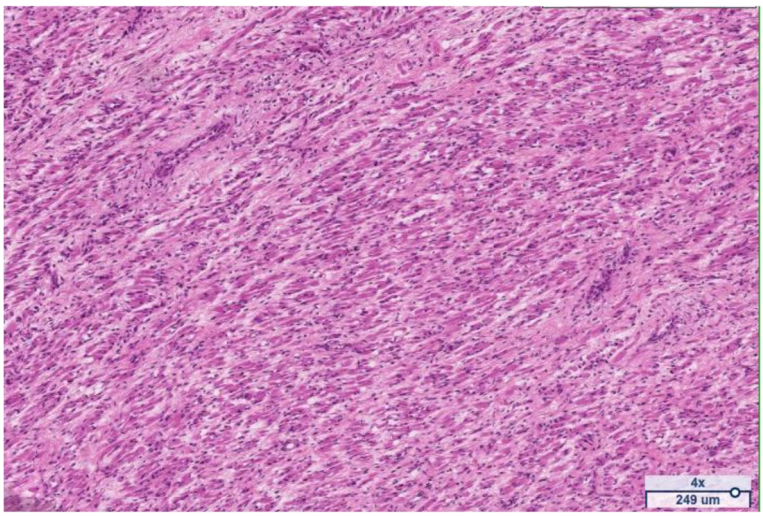

Fig. 6 Stromal WT - spindle cells arranged in short bundles (4x)

Undifferentiated pattern (blastema) of WT

This is the most important histological pattern, which must be promptly recognized by pathologists, as it is associated with a worse prognosis. It is usually composed of sheets of primitive cells that form solid areas. This pattern is part of the spectrum of "small, blue, and round" cell neoplasms, which implies several differential diagnoses that should be ruled out for proper treatment (Figs. 12 and 13).

The presence of blastema confers a worse prognosis, especially if found in surgical specimens after chemotherapy. In this situation, if the blastema represents more

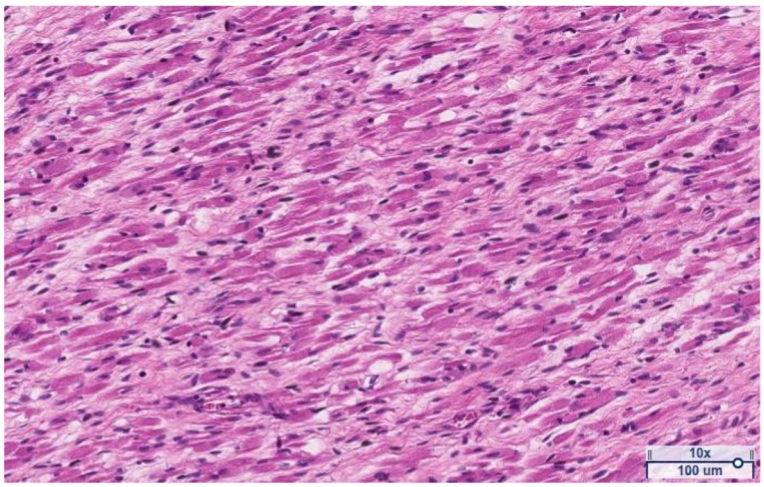

Fig. 7 Stromal WT - spindle cells arranged in short bundles with rhabdomioblastic differentiation. (10x)

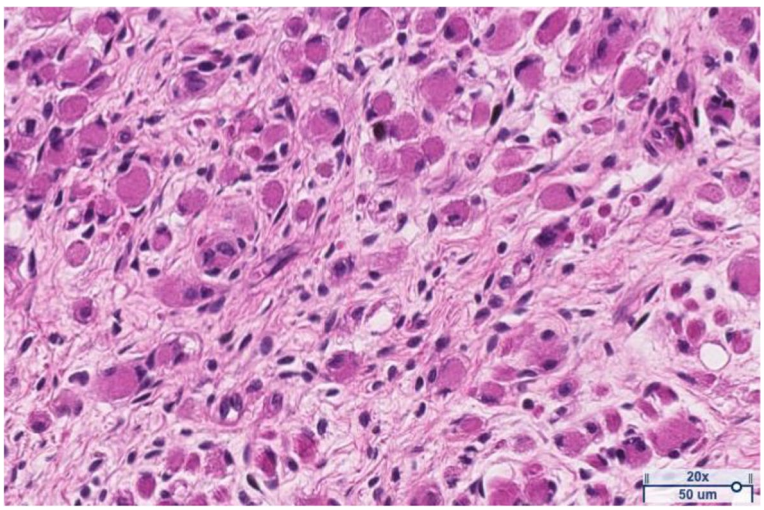

Fig. 8 Stromal WT with rhabdomyoblastic differentiation

than 66% of the residual viable component, the tumor is classified as high-risk Wilms tumor (WT), and the treatment should be intensified.

Given the microscopic patterns mentioned above, there are several other tumors whose diagnosis must be considered, as we will discuss below for each histological type of WT.

Main differential diagnosis of the epithelial pattern of WT

Metanephric adenoma (MA)

Metanephric adenoma is a benign renal neoplasm that typically affects older children. These tumors are unilateral and usually single, with well-defined borders. Macroscopically, they have a whitish cut surface with pinkish spots. Necrosis and hemorrhage are not common findings.

Histologically, metanephric adenomas consist of primitive epithelial cells arranged in acini or tubules without mitotic activity (Fig. 14). These lesions can also express wt-1 by immunohistochemistry (IHC), which does not assist in differentiating them from Wilms tumors (WT). An immunohistochemical marker of great value is CD57, which is positive in these lesions and negative in WT. The IHC expression of *BRAF* [8] and PAX-8 in metanephric adenomas also aids in the differential diagnosis from WT [9] (Table 2).

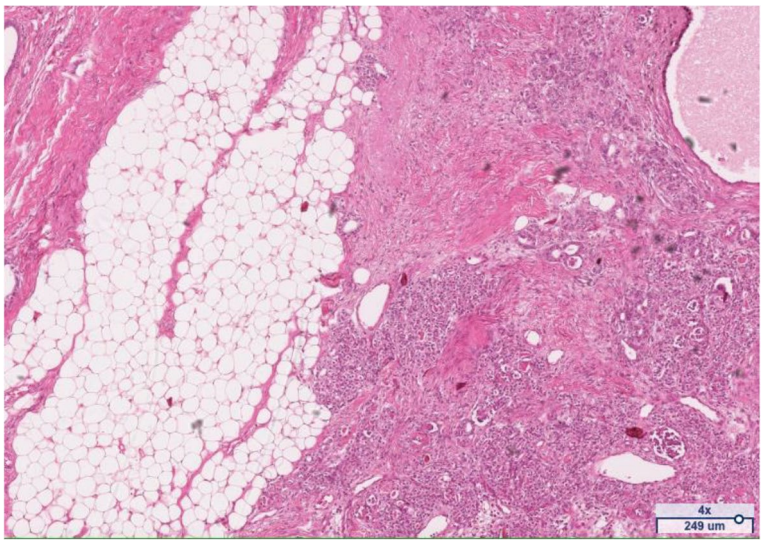

Fig. 9 Stromal WT with heterologous adipocytic component. Careful should be taken in those cases not to confuse it with renal sinus or perirenal fat invasion

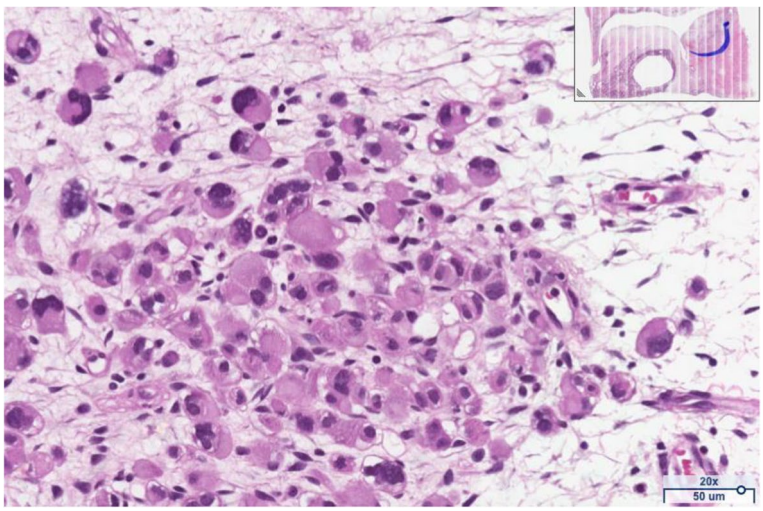

Fig. 10 Pseudoanaplasia. Areas of rhabdomyoblastic differentiation with intense pleomorphism and multinucleations. No atypical mitoses were identified

Papillary renal cell carcinoma

The epithelial pattern of WT can exhibit pseudopapillae formation (Fig. 3), which leads to a differential diagnosis with papillary renal cell carcinoma (RCC), especially in older children. The solid pattern of papillary RCC (Fig. 15) can resemble complete tubular structures, like those found in WT. The presence of other components of WT and the accumulation of histiocytes (typically present in RCC) are the primary histological findings that can aid in differentiating between the two neoplasms (Fig. 16). Immunohistochemistry can also be helpful, as papillary RCCs are negative for WT-1 and positive for AMACR and CK7 [10].

TFE-3 rearranged renal cell carcinoma

TFE-3 rearranged renal cell carcinomas can affect the pediatric age group and are therefore treated as Wilms tumors (with neoadjuvant chemotherapy before surgery) in some cases. Histologically, they are papillary tumors characterized by epithelioid cells with large, clear or eosinophilic cytoplasm and prominent nucleoli

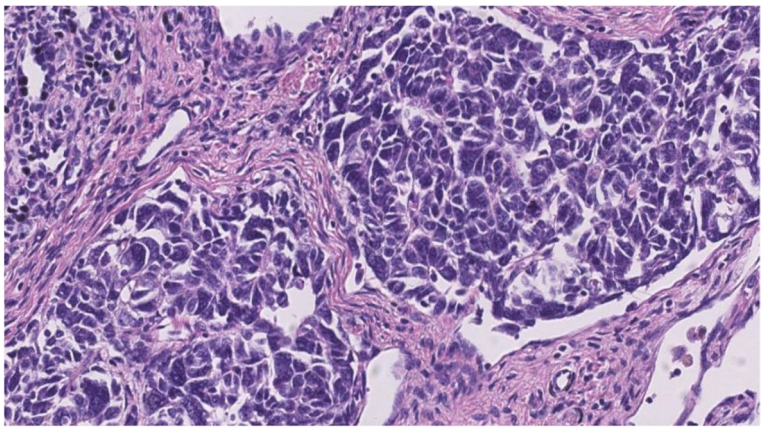

Fig. 11 Anaplasia: intense pleomorphism, multinucleation, hyperchromasia and a typical mitosis

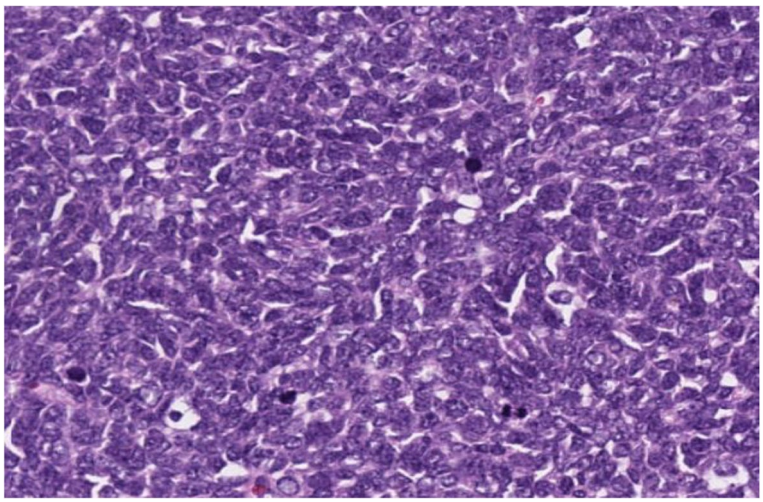

Fig. 12 Blastematous WT pattern: undifferentiated, primitive basophilic cells with scant cytoplasm, arranged in solid blocks

(Fig. 17). Psammoma bodies are frequently observed [9]. Diagnostic confirmation can be aided by the immunohistochemical expression of TFE-3, as well as cathepsin and melanocytic markers. The presence of TFE-3 rearrangement, detected by fluorescence in situ hybridization (FISH), RT-PCR, or sequencing, also confirms this diagnosis [11–13].

ALK rearrangement associated renal cell carcinoma

ALK rearrangement-associated renal cell carcinomas are very rare, accounting for less than 1% of RCC cases. These tumors are generally well-defined neoplasms and can exhibit a histological pattern similar to that of metanephric adenoma. A morphological clue is the presence of some inflammatory infiltrate at their periphery and may also include areas with mucinous stroma. These tumors are positive for PAX8 and ALK on immunohistochemistry, and the rearrangement can be confirmed using fluorescence in situ hybridization (FISH).

Cystic partially differentiated nephroblastoma

Cystic Partially Differentiated Nephroblastoma (CPDN) is defined as a completely multilocular cystic tumor primarily occurring in individuals under 2 years of age. This neoplasm features slender septa that contain aggregates of blastemal cells or epithelial immature structures.

The radiological distinction between Pediatric Cystic Nephroma (PCN), CPDN, and Cystic Wilms Tumor (CWT) presents considerable difficulties. Definitive differentiation among these three entities is only histopathological assessment, which is crucial for directing future therapeutic measures, as their biological behaviors can vary significantly.

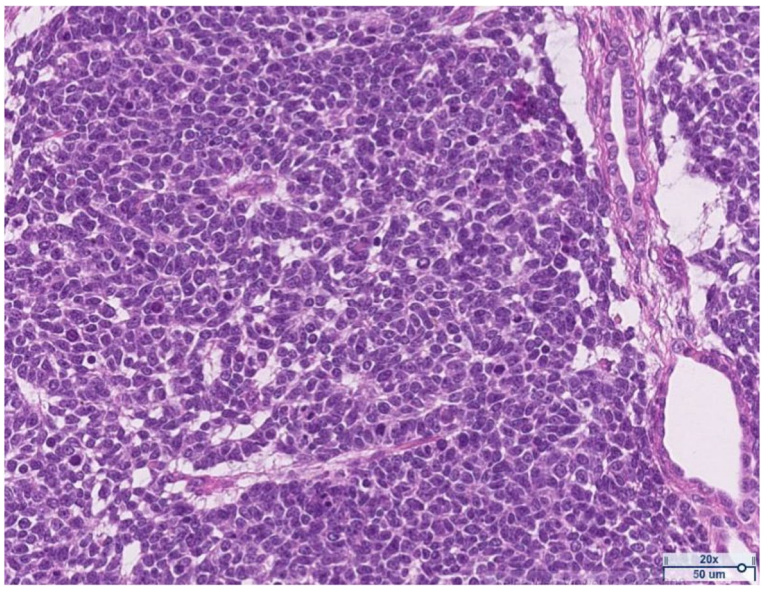

Fig. 13 WT blastematous pattern (20X)

Table 2 Main morphological, immunohistochemical (IHC) and molecular fidings among pediatric renal tumors

Tumor	Main Morphological findings	IHC	Molecular
Wilms Tumor	Triphasic tumor: epitelial, stromal and blastema	WT1 (+) CD57 (-)	WT1 mutation; TP53 mut in anaplasic cases
Metanephric adenoma	Well defined borders, primitive epithelial cells, arranged in acini or tubules, without mitosis	PAX 8 (+) CD57 (+) BRAF (+) WT1 (+)	BRAF mutation
Papillary renal cell carcinoma	Papillae áreas with histiocytes	CK7 (+) AMACR (+) WT1 (-)	MET alterations (trissomy of ch 7)
Clear Cell Sarcoma	Oval cells, with clear cytoplasm and nuclei with dispersed chromatin and imperceptible nucleoli; grouped in wide cords or nests, with the presence of vascularized septa (arboriform vessels)	BCOR(+) CCND1 (+)	BCOR mutation
MPNST	Spindle cells, with alternating hyper and hypocellular areas, with hemangiopericytic-like vascular pattern	H3K27me3 (-)	Histone methylation
Synovial sarcoma	Spindle cell are usually arranged in long fascicles, withing a stroma that ranges from collagenic to myxoid; can be biphasic, with presence of epithelial component	TLE1 (+) CD99 (+/-) WT1 (-)	t(X;18) SSX; SYT
Malignant rhabdoid tumor	Poorly differentiated neoplasms, with poorly differentiated cells, pleomorphic and eccentric nucleus, vesicular chromatin and a prominent nucleolus, with eosinophilic cytoplasm	INI 1 (-)	Loss of INI1
Neuroblastoma	Blue round cell tumor forming pseudo-rosettes	Synaptophysin (+) NSE (+)	N-MYC amplification
Ewing Sarcoma	Undifferentiated small, blue, round cells with scant cytoplasm and an inconspicuous nucleolus	CD99 (+) Fli1 (+) WT1 (-)	t(11; 22) EWS; ETS
Rhabdomyosarcoma	Blue round cell tumor, arranged in pseudoalveolar pattern or with presence of rhabdomioblats	Desmina (+) MyoD1 (+), Miogenin (+) WT1 (-)	*t*(2;13)PAX3-FOXO1 *t*(1;13) PAX7-FOXO1 (alveolar subtype)

CPDNs do not display any grossly apparent solid regions and are frequently large, appearing as multicystic tumors that can attain sizes of up to 18 cm.

Upon microscopic analysis, CPDN is categorized as a multilocular cystic tumor. The walls of the cysts predominantly encompass blastemal clusters or their epithelial

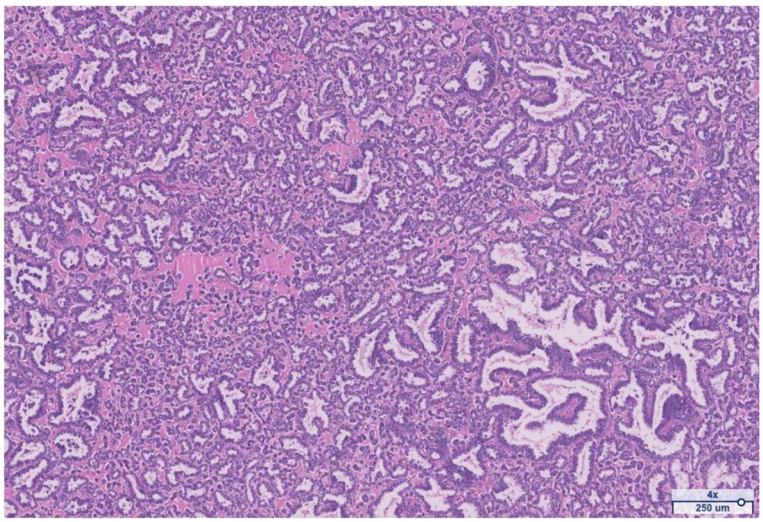

Fig. 14 Metanephric adenoma: Primitive epithelial cells, arranged in acini or tubules, without mitosis resembling epitelial WT

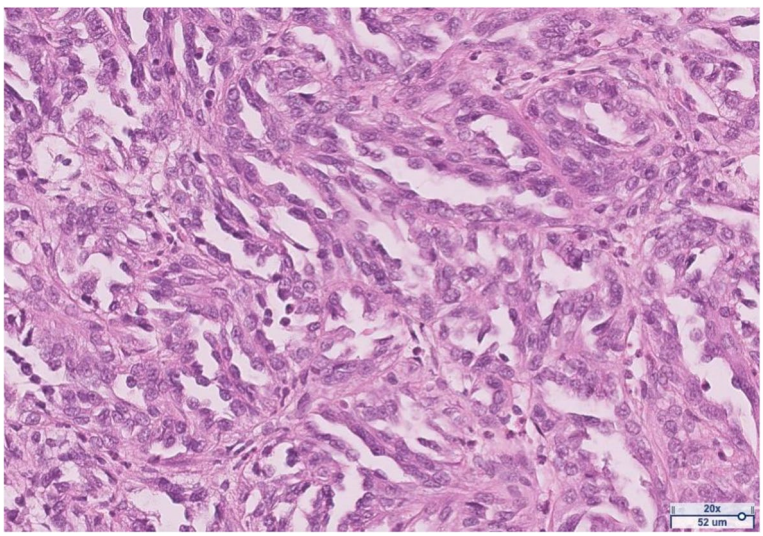

Fig. 15 Papillary renal cell carcinoma. Note the presence of accumulation of histiocytes within the neoplasm

derivatives, with sporadic mesenchymal components also noted. Importantly, there are no expansive masses that modify the smooth structure of the septa, which is different from WT.

Considering its cystic pattern, with immature structures in its septa, the differential diagnosis is primarily made with cystic Wilms tumor, as well as with cystic nephromas [14].

Cystic nephroma

Cystic nephroma (CN) is an infrequently encountered non-hereditary benign cystic tumor of the kidney. It has been referred to by various designations, predominantly multilocular cystic nephroma. Typically presenting during the first two years of life and occurring with a frequency that is twice as high in males compared to females. It represents approximately 2–3% of all primary renal tumors diagnosed in the pediatric population. The primary symptom is often an abdominal mass, as well as other renal tumors. Predominantly asymptomatic neoplasms are frequently identified incidentally through imaging studies.

Microscopic (Fig. 18) analysis reveals a neoplastic mass characterized by the presence of numerous cysts lined with cuboidal epithelium, which are demarcated by a thick septa. These lesions lack other immature

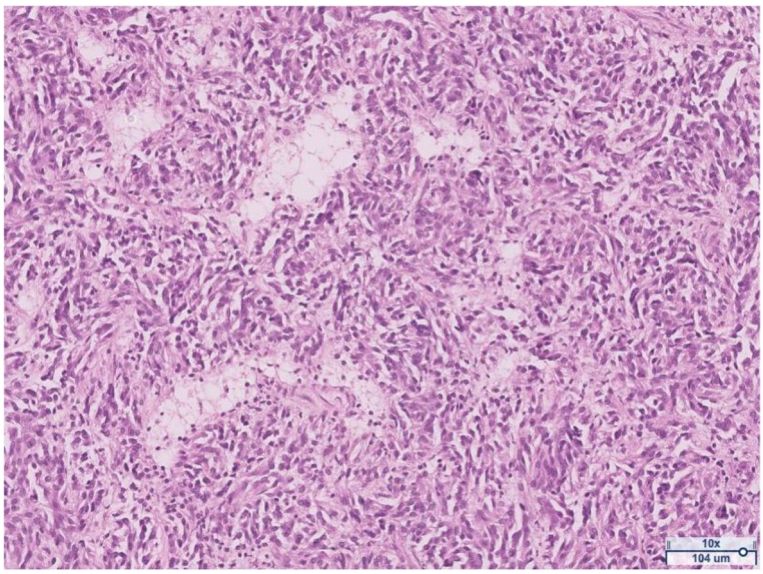

Fig. 16 Papillary renal cell carcinoma with a solid pattern, represented by tubular formations. This pattern can also be present as a epithelial pattern of WT

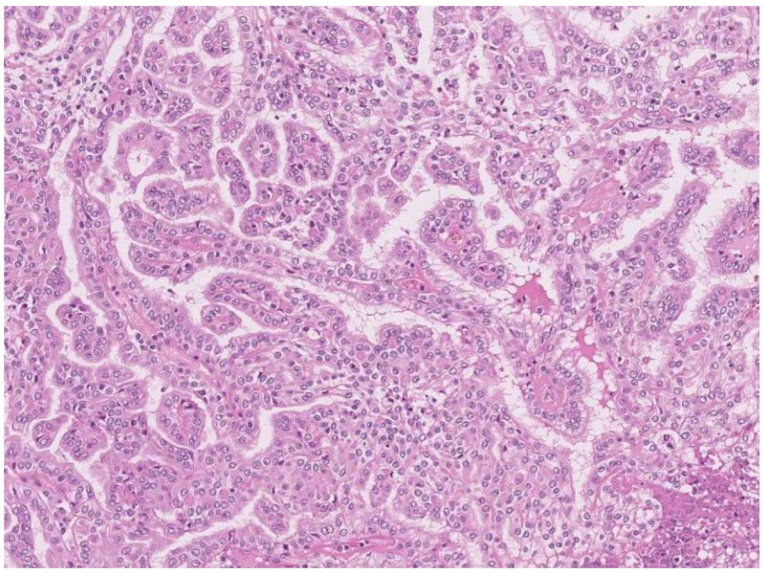

Fig. 17 TFE-3 rearranged renal cell carcinoma. Epithelioid cells with a large, clear or eosinophilic cytoplasm with evident nucleoli in a papillary rearrangement (8x)

elements within their septa, as is observed in CPDN [14].

The thickness of the septa is an important characteristic for differentiating these lesions from cystic Wilms tumors, which typically exhibit more solid areas.

The presence of mutations in the *DICER1* gene through genetic sequencing may aid in the diagnosis of CN in cases of ambiguity.

Differential diagnosis of the stromal pattern of WT

Congenital mesoblastic nephroma (CMN)

Congenital mesoblastic nephroma (CMN) is the most common renal neoplasm in children under 6 months of age. Most cases are unique and unilateral. They typically present with a solid, grayish cut surface and are composed of spindle-shaped cells without atypia. CMN

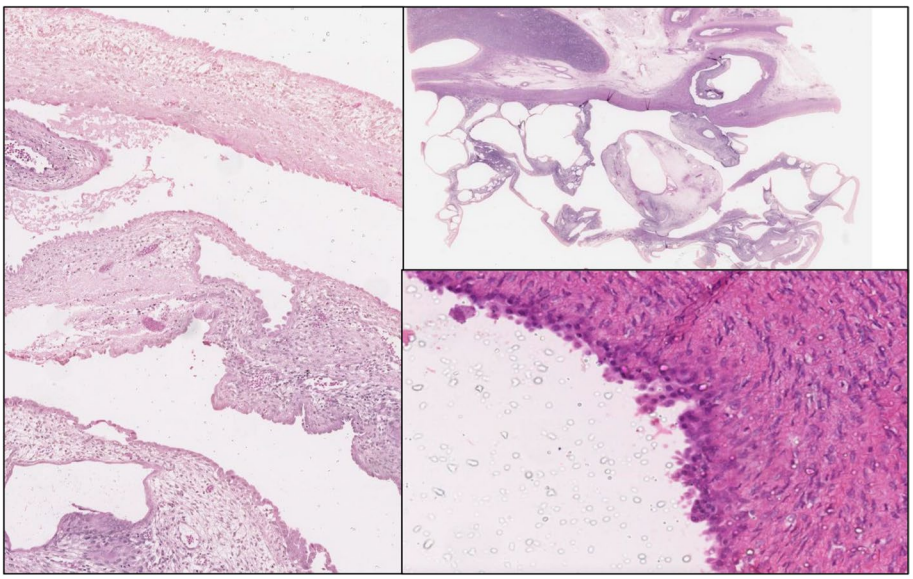

Fig. 18 Cystic nephroma: cysts lined with cuboidal epithelium, which are demarcated by a thick

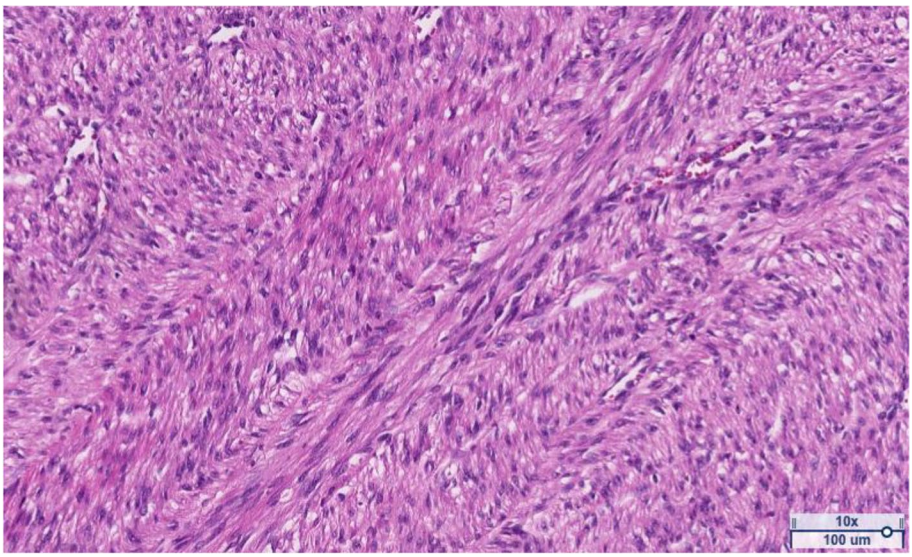

Fig. 19 Cellular type congenital mesoblastic nephroma composed of compact spindle cells, arranged in long fascicles which resemble bundles of muscle neoplasms

can be subclassified into three forms: classic, cellular (the most common), and mixed [4].

The classic type consists of spindle cells without atypia, with rare mitoses and some amount of stroma that can range from collagenous to myxoid. The cellular pattern (Fig. 19) exhibits dense cellularity, abundant mitoses, and expansive growth. The mixed type (Fig. 20) combines the other two patterns.

The molecular alteration associated with these neoplasms is the fusion of *NTRK-ETV6*, which is especially present in the cellular subtype. NTRK immunohistochemical expression can be very helpful in this diagnosis [15].

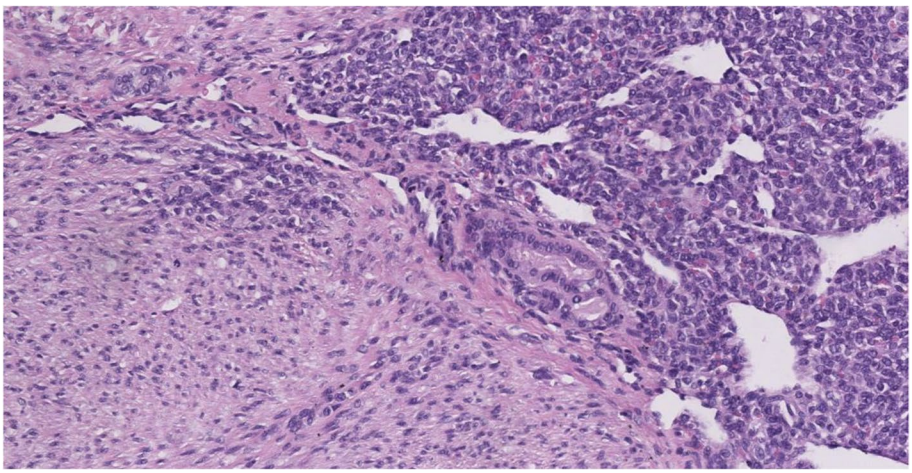

Fig. 20 Mixed-type congenital mesoblastic nephroma: note fusocellular areas of the neoplasm, allowing differential diagnosis with the stromal pattern of WT, as well as areas with rounded, basaloid and undifferentiated cells, reminiscent of the blastematous component of WT

Clear cell sarcoma of the kidney

Clear cell sarcoma of the kidney (CCSK) is the second most common renal neoplasm in the pediatric age group, accounting for 5% of childhood kidney tumors. These tumors are rare before 6 months of age, with the average age of presentation being 3 years. Clinically, patients typically seek medical attention due to the presence of a palpable abdominal mass, like Wilms tumors (WT). Frequent sites of metastasis include lymph nodes, bone, lungs, and retroperitoneum.

Macroscopically, CCSKs appear as whitish lesions with a "fish flesh" appearance.

Microscopically, CCSK can exhibit a broad spectrum of patterns. The most common pattern features oval cells with clear cytoplasm and nuclei displaying dispersed chromatin and imperceptible nucleoli. These cells are grouped in wide cords or nests, with the presence of vascularized septa (arboriform vessels) [9]. CCSK may also present with myxoid, sclerosing, and epithelioid patterns (Figs. 21, 22, 23 and 24).

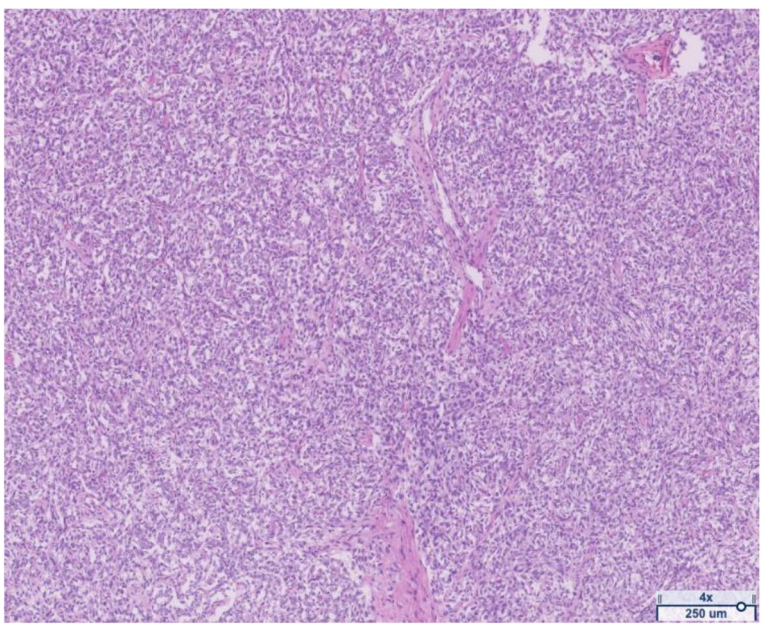

Fig. 21 Clear cell sarcoma of the kidney. Presence of oval cells, with clear cytoplasm and nuclei with dispersed chromatin and imperceptible nucleoli (4x)

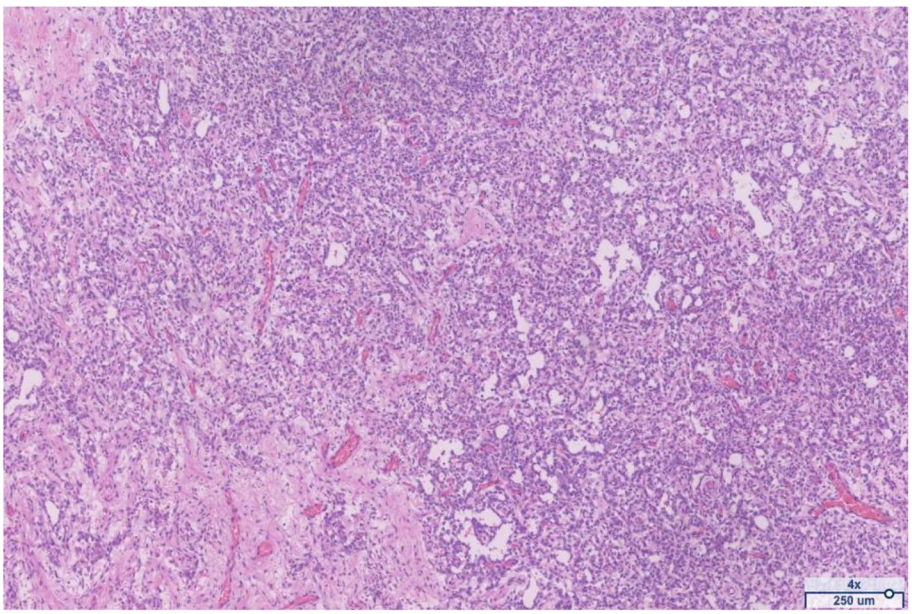

Fig. 22 Clear cell sarcoma of the kidney: Presence of oval cells, with clear cytoplasm and nuclei with dispersed chromatin and imperceptible nucleoli (4x)

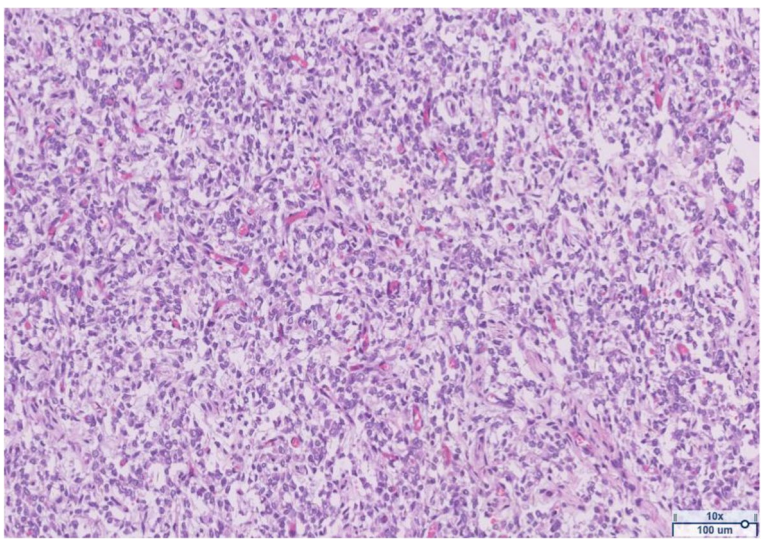

Fig. 23 Clear cell sarcoma of the kidney with clear cytoplasm and arboriform fibrovascular septa between the cells (20x)

Immunohistochemically, these tumors show positivity for BCOR and cyclin D1, and negativity for CD34, S100, desmin, and cytokeratins [16]. CCSK is staged in the same manner as Wilms tumors (WT).

Malignant peripheral nerve sheath tumor (MPNST)

Malignant peripheral nerve sheath tumor (MPNST) is a malignant neoplasm that originates in peripheral nerves and is primarily composed of spindle cells. These tumors appear in children, mainly in the context of neurofibromatosis. Histologically, MPNSTs consist of spindle cells arranged in alternating hypercellular and hypocellular areas, displaying a hemangiopericytic-like vascular pattern.

When these tumors are located in the renal region, they pose a challenge for differential diagnosis with stromal Wilms tumors (WT) and may also contain heterologous components such as bone, cartilage, and skeletal muscle (TRITON tumors – Fig. 25) [9], which complicates their differentiation from WT. More recently, MPNSTs have

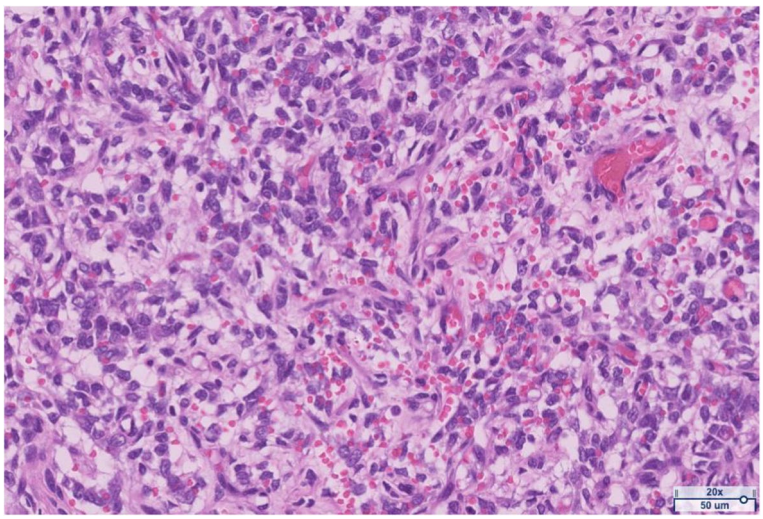

Fig. 24 Clear cell sarcoma of the kidney with clear cytoplasm and arboriform fibrovascular septa between the cells (20x)

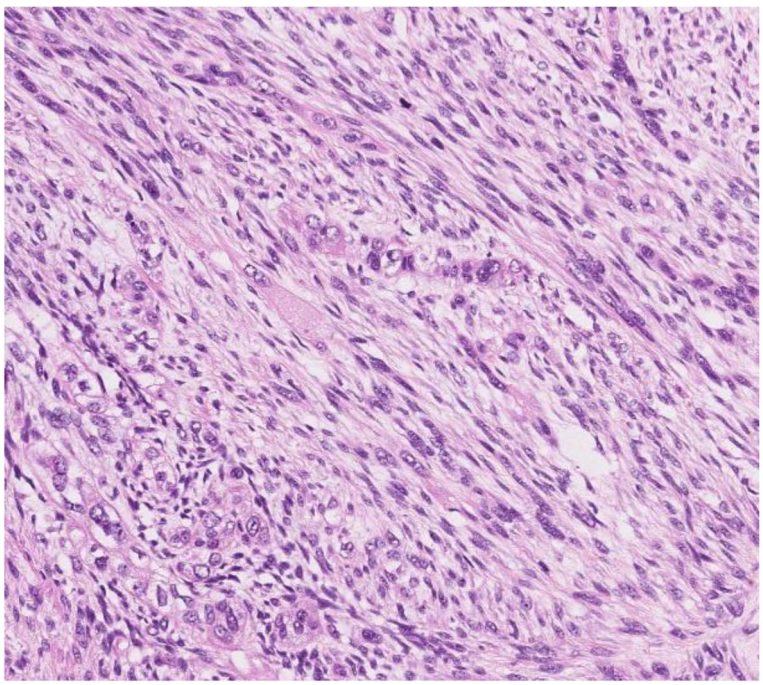

Fig. 25 MPNST with rhabdomioblastic differentiatin (TRITON tumor) (20x) (10x)

been associated with histone methylation, leading to the detection of loss of trimethylated histone (H3K27me3) [17] by immunohistochemistry [18], which helps establish the diagnosis.

Synovial sarcoma (SS)

Synovial sarcoma (SS) is a high-grade spindle cell or undifferentiated sarcoma that primarily affects the limbs of young adults but can also be found as visceral tumors. SS in children is rare, particularly as a kidney tumor, with only case reports or small series described in the literature [19]. SS can be monophasic, exhibiting a pure fusocellular pattern, or biphasic, where an epithelial component is found among the spindle cell component. The spindle cells are typically arranged in long fascicles within a stroma that ranges from

collagenous to myxoid. The cells tend to be uniform, with little cytoplasm, ovoid nuclei, and inconspicuous nucleoli. Mitoses are variable, and pleomorphism is not present. Many cases exhibit a vascular pattern resembling staghorn neoplasia.

SS has a t(x;18)(p11;q11) translocation, in which the SS18 gene on chromosome 18 is fused with the *SSX* gene on the X chromosome. This rearrangement can be detected by FISH, RT-PCR, or sequencing, and its presence is pathognomonic of SS.

Histological changes induced by neoadjuvant chemotherapy

Wilms tumors that are treated with neoadjuvant chemotherapy using the SIOP protocol can exhibit areas rich in inflammatory reactions and histiocytes (Fig. 26), necrosis (Fig. 27), hemorrhage, and fibrosis. The objective of this treatment is to reduce tumor size, encapsulate the neoplasm (thereby facilitating surgical procedures), and decrease the amount of viable neoplasia. Among the three histological patterns of Wilms tumors, the blastema pattern is the one that responds most effectively to chemotherapy.

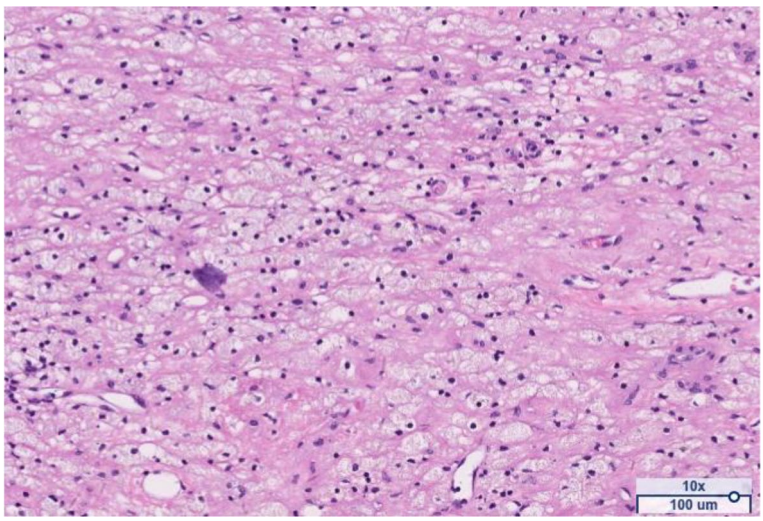

Fig. 26 Area of response to chemotherapy with abundant histiocytic infiltration

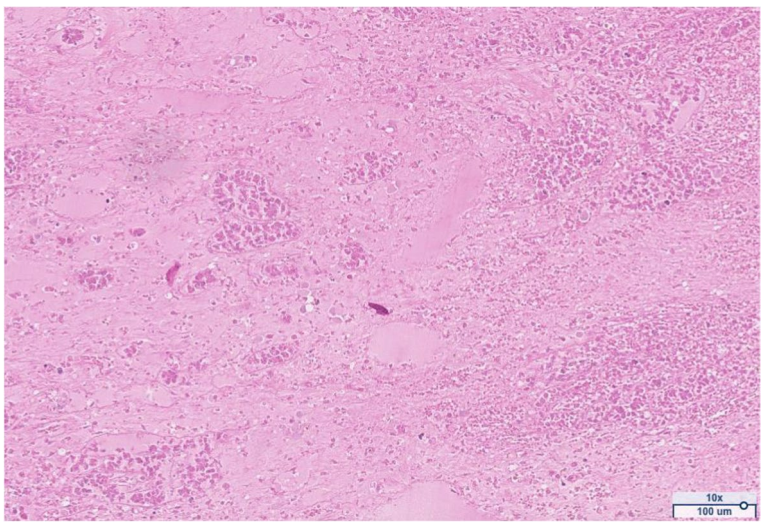

Fig. 27 Chemotherapy response area: necrotic areas (10x)

It is not uncommon for areas of response to be misinterpreted as viable stromal areas of Wilms tumors (WT), as fibrosis can be easily confused with these areas.

The areas of chemotherapy response are critical for the appropriate quantification of viable and non-viable neoplasia, as accounting for non-viable regions as viable can skew percentage calculations, subsequently influencing patient risk. Non-viable neoplastic thrombi result in the child's staging being classified as stage 3; therefore, the re-recognition of non-viable neoplasia in these regions is essential.

Differential diagnosis of the blastema pattern of WT

Malignant rhabdoid tumor

Malignant rhabdoid tumor is another rare renal neoplasm, accounting for less than 2% of cases, that occurs in pediatric patients, averaging 1 year of age. These tumors are generally silent, large, and highly aggressive.

In these tumors, the *SMARCB1 (INI1)* gene is inactivated due to mutations, deletions, or loss of heterozygosity [19].

Microscopically, they are poorly differentiated neoplasms characterized by pleomorphic cells with eccentric nuclei, vesicular chromatin, and prominent nucleoli, accompanied by eosinophilic cytoplasm (Fig. 28). The growth patterns can vary and may include solid, sclerosing, epithelioid, spindle cell, or even cystic areas. These tumors are usually extensively necrotic.

The immunohistochemical study is highly sensitive and specific when using the INI-1 antibody, which is negative (lost) in malignant rhabdoid tumors [9].

Neuroblastoma

Neuroblastoma is defined as a malignant tumor derived from the cells of the primordial neural crest, making it the third most common tumor in childhood, with an average age of diagnosis at 5 years. Clinically, the child presents with elevated catecholamines, which can aid in differential diagnosis. It usually affects the adrenal gland, but in cases of large masses, it can involve the kidney, making it difficult to differentiate its boundaries using imaging methods. Rarely, it can originate from the kidney.

Microscopically, the undifferentiated and poorly differentiated subtypes require a differential diagnosis with the blastema component of Wilms tumor (WT), since the blastema pattern of nephroblastoma can exhibit primitive tubular structures or pseudo-rosettes (Fig. 29), like those found in neuroblastomas [4]. Immunohistochemical studies (showing positivity for synaptophysin and enolase) and molecular studies (indicating the presence of NMYC amplification) assist in the diagnosis, as these traits are characteristic of neuroblastoma and are not found in WT.

Ewing sarcoma

Ewing Sarcoma is common in adolescents and young adults, with 80% of cases occurring in individuals under 20 years of age. It is an aggressive neoplasm with a poor prognosis, especially if it does not respond to chemotherapy. While many cases affect the bones, about 12% are extra skeletal [9]. Visceral tumors are rare, with only a few cases reported in literature [20]. Microscopically, this neoplasm is characterized by undifferentiated small, blue, round cells (Figs. 30 and 31), which have scant cytoplasm and an inconspicuous nucleolus [9].

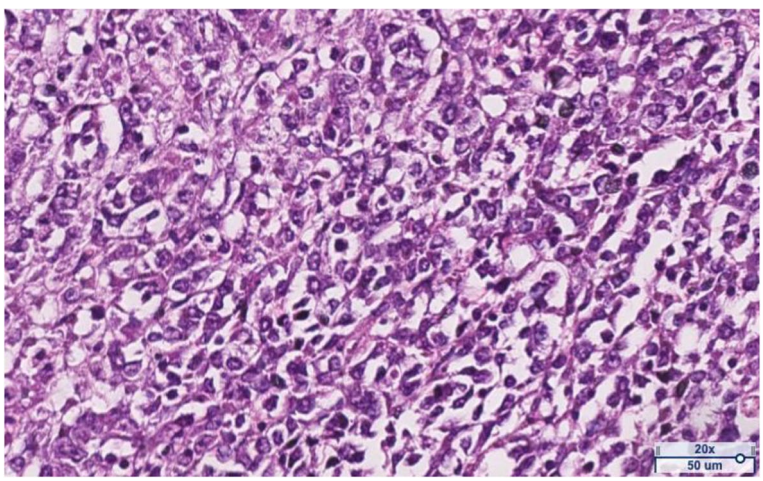

Fig. 28 Malignant rhabdoid tumor: poorly differentiated neoplasms, with poorly differentiated cells, pleomorphic and eccentric nucleus, vesicular chromatin and a prominent nucleolus, with eosinophilic cytoplasm (20x)

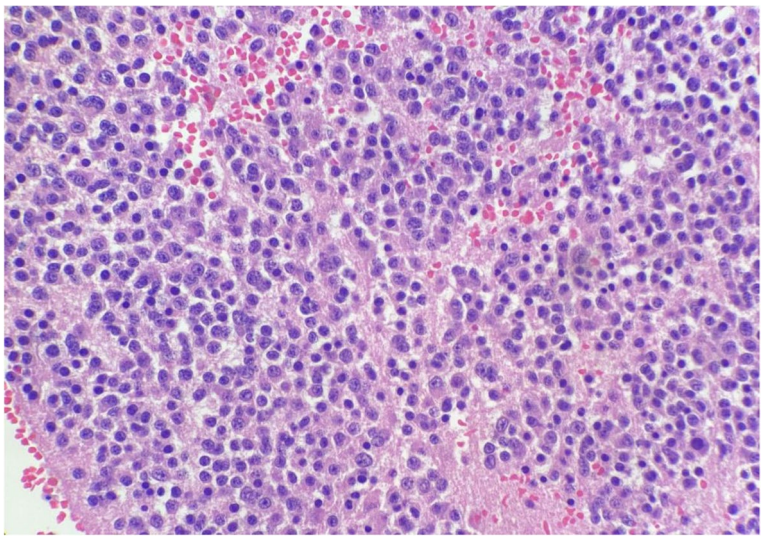

Fig. 29 Neuroblastoma, composed of primitive small blue and round cells, similar to blastema component of TW (20x)

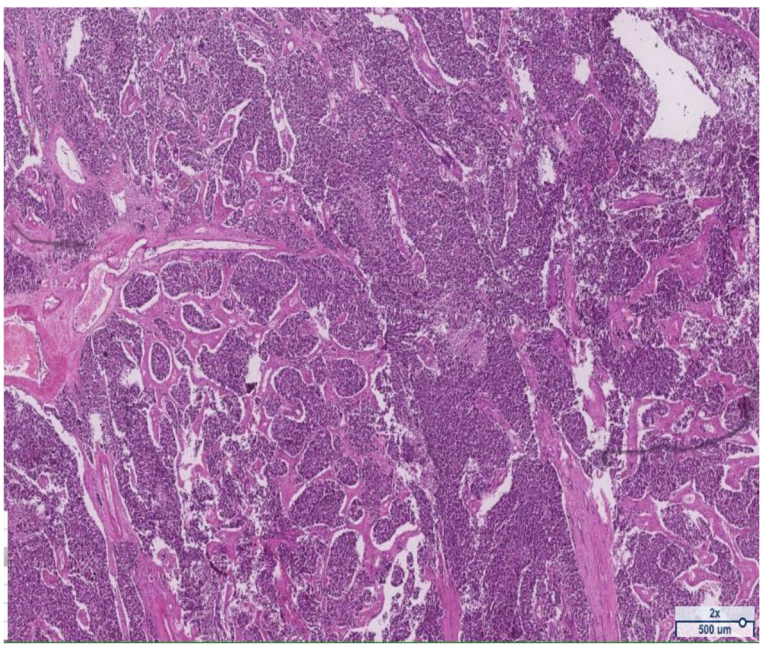

Fig. 30 Ewing sarcoma: aggressive malignant neoplasm characterized by the presence of small, blue, round cells

Immunohistochemical (IHC) expression typically shows positivity for CD99, FLI-1, and ERG, although the expression of cytokeratin can also be present. Ewing sarcomas are genetically characterized by fusions involving EWS genes and genes from the ETS family. The detection of these genetic fusion aids in diagnosis.

Rhabdomyosarcoma

Like Ewing's sarcoma, rhabdomyosarcoma (RMS) is an aggressive neoplasm that affects children and young adults, presenting as either limb or visceral tumors. There are two main types found in children: alveolar rhabdomyosarcoma (ARMS) and embryonal rhabdomyosarcoma (ERMS). ARMS is more prevalent in adolescents

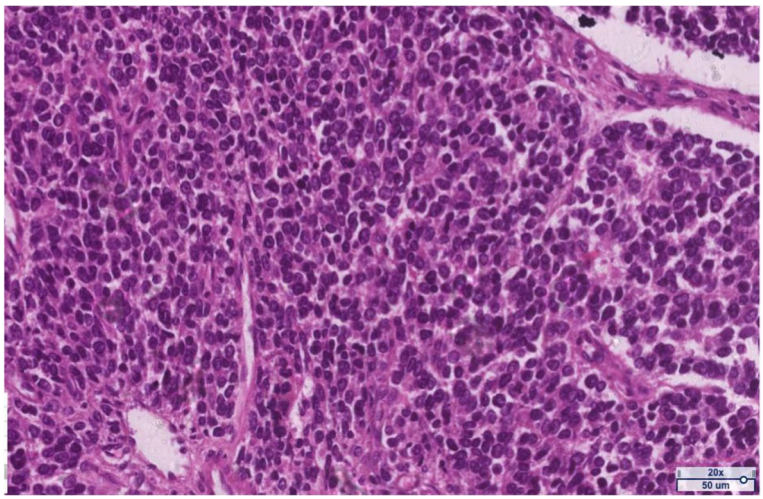

Fig. 31 Ewing sarcoma: aggressive malignant neoplasm characterized by the presence of small, blue, round cells

and young adults and histologically presents with small, round cells arranged in pseudo-alveolar formations, separated by fibrous septa.

ERMS is more common in younger children and often presents in the genitourinary system. Histologically, it can range from undifferentiated cells to well-differentiated cells (rhabdomyoblasts), which can be easily identified. The cells can be distributed within a myxoid stroma or exhibit a more compact, solid arrangement [9].

Both types are mesenchymal lesions with muscle differentiation, so muscle differentiation markers that can be detected by IHC, such as desmin, myogenin, and MyoD1, are helpful in diagnosis. Molecularly, ARMS is associated with the PAX-FOXO-1 fusion. The treatment of these tumors differs from that of Wilms tumor (WT), as there are targeted drugs for RMS, including ATR, KDM4B, and PDGFRA inhibitors [21].

Conclusion

Wilms tumors are rare neoplasms that require differential diagnosis with other kidney tumors, especially when they do not exhibit all three histological components. Therefore, understanding its differential diagnosis is crucial for the effective treatment of these tumors, highlighting the importance of having trained pathologists specializing in pediatric and childhood neoplasms.

Abbreviations

ARMS	Alveolar rhabdomyosarcoma
CCSK	Clear cell sarcoma of the kidney
CMN	Congenital mesoblastic nephroma
CN	Cystic nephroma
CPDN	Cystic Partially Differentiated Nephroblastoma
COG	Children's Oncology Group
ERMS	embryonal rhabdomyosarcoma
GCBTTW	Grupo Brasileiro de Tumores Renais
GBTR	Grupo Brasileiro de Tumores Renais
IHC	Immunohistochemestry
LO	Laboratório de origem
LRC	laboratório de revisão central
MPNST	Malignant peripheral nerve sheath tumor
NWTS	National Wilms Tumor Study
RMS	rhabdomyosarcoma
RTSG	Renal Tumor Study Group
RCC	Renal cell carcinoma
rt	PCR-Real time polymerase chain reaction
SS	Synovial sarcoma
SIOP	Société Internationale d´Oncologie Pédiatrique
SCC	Sarcoma de células claras
SOBOPE	Sociedade Brasileira de Oncologia Pediátrica
WT	Wilms Tumor

Authors' contributions

All authors read and approved the final manuscript.

Funding

This research did not receive any specific grant from funding agencies in the public, commercial, or not-for-profit sectors.

Data availability

The datasets used and/or analyzed during the current study are available from the corresponding author on reasonable request.

Declarations

Ethics approval and consent to participate

This study was submitted and approved by the Research Ethics Committee of UNIFESP – Hospital São Paulo, SP, Brazil (CEP) under number CAAE: 52281416.8.1001.5505. The "Free and Informed Consent Form" (TCLE) was not necessary for patients, as this research is retrospective in nature, as it involves collecting data from medical records and it is not possible to contact the selected research subjects. The author undertakes to preserve the privacy of research subjects, ensuring that the data collected will be used solely and exclusively for the execution of the project in question, and that the information disclosed in no way identifies the research subject.

Competing interests

The authors declare no conflict of interest.

Received: 22 August 2024 Accepted: 24 October 2024
Published online: 20 November 2024

References

1. Vujanić GM, Sandstedt B, Kelsey A, Sebire NJ. Central pathology review in muiticenter trials and studies. Cancer. 2009;115(9):1977–83.
2. Sebire NJ, Vujanic GM. Paediatric renal tumours: recent developments, new entities and pathological features. Histopathology. 2009;54(5):516–28.
3. Vujanić GM, Gessler M, Ooms AHAG, Collini P, Coulomb-l'Hermine A, D'Hooghe E, et al. The UMBRELLA SIOP–RTSG 2016 Wilms tumour pathology and molecular biology protocol. Nature Reviews Urology. Volume 15. Nature Publishing Group; 2018. pp. 693–701.
4. van den Heuvel-Eibrink MM, editor. Wilms Tumor. Codon; 2016.
5. Vujani? GM, Harms D, Sandstedt B, Weirich A, de Kraker J, Delemarre JFM. New definitions of focal and diffuse anaplasia in Wilms tumor: the International Society of Paediatric Oncology (SIOP) experience. Med Pediatr Oncol. 1999;32(5):317–23.
6. Mifsud W, Furtwängler R, Vokuhl C, D'Hooghe E, Pritchard-Jones K, Graf N, et al. Treatment of patients with stage I focal anaplastic and diffuse anaplastic Wilms tumour: a report from the SIOP-WT-2001 GPOH and UK-CCLG studies. Eur J Cancer. 2022;166:1–7.
7. Vujanić GM, Mifsud W, Chowdhury T, Al-Saadi R, Hons B, Pritchard-Jones K. Characteristics and outcomes of preoperatively treated patients with anaplastic Wilms tumors registered in the UK SIOP-WT-2001 and IMPORT study cohorts (2002–2020). Cancer. 2022;128(8):1666–75. Available from: https://acsjournals.onlinelibrary.wiley.com/doi/10.1002/cncr.34107. Cited 2024 Jan 22
8. Pinto A, Signoretti S, Hirsch MS, Barletta JA. Immunohistochemical staining for BRAF V600E supports the diagnosis of metanephric adenoma. Histopathology. 2015;66(6):901–4. Available from: https://onlinelibrary.wiley.com/doi/full/10.1111/his.12509. Cited 2024 Jan 10
9. Cree AI, Goldman-Levy G, Lokuhetty D, Rao B, White V VA, editors. WHO classification of Tumours Editorial Board. Urinary and male genital tumours. Volume 8, 5th ed. Lyon: International Agency for Research on Cancer; 2022.
10. Delahunt B, Eble JN. Papillary renal cell carcinoma: a clinicopathologic and immunohistochemical study of 105 tumors. Mod Pathol. 1997;10(6):537–44.
11. Green WM, Yonescu R, Morsberger L, Morris K, Netto GJ, Epstein JI, et al. Utilization of a TFE3 break-apart FISH assay in a renal tumor Consultation Service. Am J Surg Pathol. 2013;37(8):1150–63.
12. Argani P, Lal P, Hutchinson B, Lui MY, Reuter VE, Ladanyi M. Aberrant nuclear immunoreactivity for TFE3 in Neoplasms with TFE3 gene fusions. Am J Surg Pathol. 2003;27(6):750–61.
13. Martignoni G, Pea M, Gobbo S, Brunelli M, Bonetti F, Segala D, et al. Cathepsin-K immunoreactivity distinguishes MiTF/TFE family renal translocation carcinomas from other renal carcinomas. Mod Pathol. 2009;22(8):1016–22.
14. van Peer SE, Pleijte CJH, de Krijger RR, Jongmans MCJ, Kuiper RP, Lilien MR, et al. Clinical and molecular characteristics and outcome of cystic partially differentiated Nephroblastoma and cystic Nephroma: a narrative review of the literature. Cancers (Basel). 2021;13(5):997.
15. Argani P, Fritsch M, Kadkol SS, Schuster A, Beckwith JB, Perlman EJ. Detection of the ETV6-NTRK3 chimeric RNA of Infantile Fibrosarcoma/Cellular congenital mesoblastic Nephroma in paraffin-embedded tissue: application to Challenging Pediatric Renal stromal tumors. Mod Pathol. 2000;13(1):29–36.
16. Wong MK, Ng CCY, Kuick CH, Aw SJ, Rajasegaran V, Lim JQ, et al. Clear cell sarcomas of the kidney are characterised by BCOR gene abnormalities, including exon 15 internal tandem duplications and BCOR-CCNB3 gene fusion. Histopathology. 2018;72(2):320–9.
17. Pekmezci M, Cuevas-Ocampo AK, Perry A, Horvai AE. Significance of H3K27me3 loss in the diagnosis of malignant peripheral nerve sheath tumors. Mod Pathol. 2017;30(12):1710–9.
18. Schaefer IM, Dong F, Garcia EP, Fletcher CDM, Jo VY. Recurrent SMARCB1 inactivation in Epithelioid malignant peripheral nerve sheath tumors. Am J Surg Pathol. 2019;43(6):835–43.
19. Fisher C, Folpe AL, Hashimoto H, Weiss SW. Intra-abdominal synovial sarcoma: a clinicopathological study. Histopathology. 2004;45(3):245–53.
20. Grünewald TGP, Cidre-Aranaz F, Surdez D, Tomazou EM, de Álava E, Kovar H, et al. Ewing sarcoma. Nat Rev Dis Primers. 2018;4(1):5.
21. Haase GM, O'Leary MC, Stram DO, Lukens JN, Seeger RC, Shimada H, et al. Pelvic neuroblastoma—implications for a new favorable subgroup: a Children's cancer group experience. Ann Surg Oncol. 1995;2(6):516–23.

Publisher's Note